

Efficient Online Computation of Business Process State From Trace Prefixes via N-Gram Indexing

David Chapela-Campa, *University of Tartu, Estonia*, david.chapela@ut.ee
 Marlon Dumas, *University of Tartu, Estonia*, marlon.dumas@ut.ee

Abstract—This paper addresses the following problem: Given a process model and an event log containing trace prefixes of ongoing cases of a process, map each case to its corresponding state (i.e., marking) in the model. This state computation operation is a building block of other process mining operations, such as log animation and short-term simulation. An approach to this state computation problem is to perform a token-based replay of each trace prefix against the model. However, when a trace prefix does not strictly follow the behavior of the process model, token replay may produce a state that is not reachable from the initial state of the process. An alternative approach is to first compute an alignment between the trace prefix of each ongoing case and the model, and then replay the aligned trace prefix. However, (prefix-)alignment is computationally expensive. This paper proposes a method that, given a trace prefix of an ongoing case, computes its state in constant time using an index that represents states as n-grams. An empirical evaluation shows that the proposed approach has an accuracy comparable to that of the prefix-alignment approach, while achieving a throughput of hundreds of thousands of traces per second.

Index Terms—process mining, state computation, n-gram index, short-term simulation, log animation

I. INTRODUCTION

PROCESS MINING (PM) is a set of techniques to discover, analyze, simulate, and monitor processes to optimize their performance, using event logs representing the execution of cases in a process [1]. Several PM operations require us to determine the state of each ongoing case of a process, i.e., which activities may be executed next according to a process model. The state of all ongoing cases is needed, for example, for log animation [2], to resume the visual replay of cases whenever the user advances the cursor to an arbitrary point in the log’s timeframe. Similarly, in short-term (online) simulation [3]–[5], the state of each case needs to be determined to simulate the remainder activities of those cases.

In these settings, the problem of state computation may be defined as follows: Given a process model and an event log containing ongoing cases of a process, map each case to its corresponding state (i.e., marking) in the model. Note that the trace prefix of an ongoing case may not perfectly fit the model, or it may lead to multiple equally possible markings. For example, given the process model in Figure 1a, and the running case ⟨Register invoice, Notify, Post invoice, Notify⟩, both markings {5, 8} and {4, 8} are correct answers to the state computation problem. The execution may loop back via either flow 9 or flow 12 to fire the second instance of “Notify”.

This state computation problem can be approached by replaying the trace prefix on the process model [6], [7].

However, in the case of non-fitting traces, i.e., traces with deviations from the behavior supported by the process model, (token-based) replay approaches produce markings that are not reachable from the start state. This issue can be addressed by computing an optimal alignment between the trace prefix and the process model [8], and then performing the replay using the resulting alignment. However, both the prefix alignment and the prefix replay step have exponential complexity. In log animation or short-term simulation, there is a need to compute the state of thousands of ongoing cases in interactive times, which requires a method with low online complexity.

This paper proposes a method to compute the state of an ongoing case, given its trace prefix, in constant time. The key idea is that the last n executed activities (n being a tunable parameter) are often sufficient to identify the current marking of an ongoing case. Accordingly, the method builds the reachability graph of the process model and creates an index that maps the ending n -gram (i.e., last n activities) of every possible trace prefix generated by the model, to the state(s) this prefix leads to. The index is created offline. At runtime, the state of an ongoing case is computed in constant time by searching for the ending n -gram in the index.

The paper reports on an evaluation of the proposed method to assess: *i*) its ability to accurately compute the already-known state of ongoing cases, *ii*) its accuracy in real-life scenarios where the state of the process is unknown, and *iii*) its efficiency. The evaluation relies on 6 synthetic event logs with different levels of noise and 12 event logs of real-life processes.

The rest of the paper is structured as follows. Sec. II introduces background concepts on process mining and state computation. Sec. III reviews related work. Sec. IV describes the proposed method. Finally, Sec. V discusses the evaluation, and Sec. VI draws conclusions and sketches future work.

II. BACKGROUND

We consider a process involving a set of *activities* A . An *event* $\varepsilon = (\varphi, \alpha, \tau)$ denotes an instance of activity $\alpha \in A$, where φ identifies the *case* to which this event belongs, and τ denotes the timestamp of this event.¹ A *trace* is a sequence of events $\langle \varepsilon_1, \varepsilon_2, \dots, \varepsilon_n \rangle$ with a common case identifier (φ). We may represent a trace in simplified form as a sequence of activities sorted chronologically, e.g., ⟨A, B, C⟩. An *event*

¹We work with a type of event log known as activity instance log, where there is one entry per activity instance and each activity instance has one timestamp (its end time).

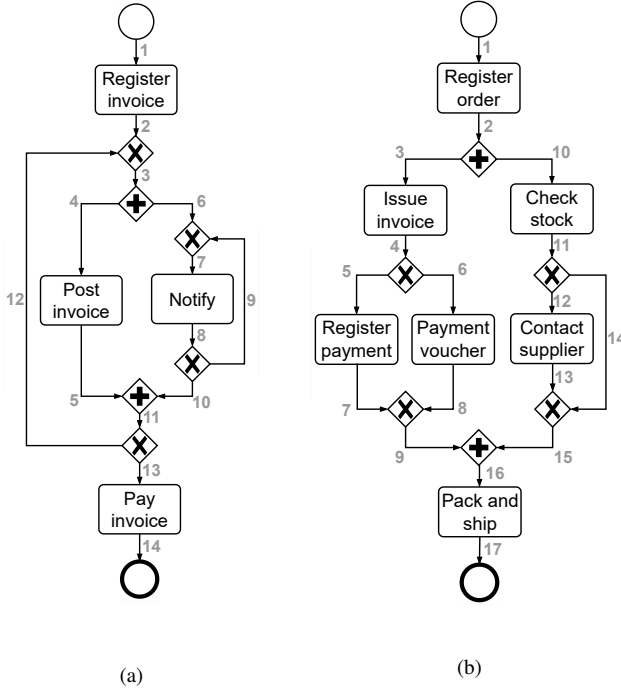


Figure 1. Workflow graphs of invoicing (a) and order handling (b) processes.

\log is a collection of traces. A (case) variant is a unique activity sequence, and its *frequency* is the number of cases whose corresponding traces match this activity sequence.

Given a set of *final activities* $FA \subseteq A$ designated by a user, an *ongoing case* is a case where the most recent activity is not in FA . The trace of an ongoing case is called its *trace prefix*.

At an abstract level, a *process model* is a graphical representation of the set of traces of a process. There are many formalisms to represent process models, e.g., BPMN² and Petri nets [9]. In this paper, we represent process models as *Workflow graphs*, which correspond to a subset of BPMN [10].

Definition 1 (Workflow graph, based on [10]). A Workflow graph $W = (source, sink, N, F, c, l)$ consists of a start event *source*, an end event *sink*, a set N of nodes, a set F of flows, a mapping $c : F \rightarrow (\{source\} \cup N) \times (N \cup \{sink\})$ that maps each flow to an ordered pair of two elements, the first one – i.e., the source – being the start event or a node, and the second one – i.e., the target – being the end event or a node, and a mapping $l : N \rightarrow \{AND, XOR, task\}$ that assigns a *logic* to every node $n \in N$; such that *i)* *source* and *sink* have, respectively, one single outgoing and one single incoming flow, *ii)* for each node $n \in N$ there exists a path from *source* to *sink* that includes n , and *iii)* a node of type “task” always has a single incoming flow and a single outgoing flow. Finally, for a node $n \in N$, the set of incoming flows is denoted by $\bullet n$, and the set of outgoing flows by $n \bullet$; and $source \bullet$ and $\bullet sink$ denote, respectively, the sets with the outgoing flow of *source* and the incoming flow of *sink*.

Figure 1 depicts two workflow graphs. The thin-lined and

Table I
EXAMPLE OF TOKEN-REPLAY SEMANTICS OVER THE BPMN MODEL IN
FIGURE 1B.

| Current state | Enabled nodes | Firing node |
|---------------|-------------------------------------|------------------|
| {1} | {Register order} | Register order |
| {2} | {AND-split} | AND-split |
| {3, 10} | {Issue invoice, Check stock} | Check stock |
| {3, 11} | {Issue invoice, right-XOR-split} | Issue invoice |
| {4, 11} | {left-XOR-split, right-XOR-split} | left-XOR-split |
| {5, 11} | {Register payment, right-XOR-split} | Register payment |
| {7, 11} | {left-XOR-join, right-XOR-split} | left-XOR-join |
| {9, 11} | {right-XOR-split} | right-XOR-split |
| {9, 12} | {Contact supplier} | Contact supplier |
| {9, 13} | {right-XOR-join} | right-XOR-join |
| {9, 15} | {AND-join} | AND-join |
| {16} | {Pack and ship} | Pack and ship |
| {17} | {{SINK}} | - |

the thick-lined circles represent, respectively, the start and end events. They indicate in which state the process starts, and in which state it ends. A rectangle represents a “task” node. A diamond-shaped node represents a *gateway*. Gateways capture the routing logic in the process. There are two types of gateways: “AND” gateways, represented by a “plus” symbol, and an “XOR” gateway, represented by a “cross” symbol. Orthogonally to the type of gateway (XOR or AND), a gateway with multiple incoming edges is called a *join*, and a gateway with multiple outgoing edges is called a *split*. Without loss of generality, we assume that a gateway is either a split or a join. A gateway that is both a split and a join can be rewritten into a join gateway followed by a split gateway. With this assumption, there are four types of gateways: XOR-split, XOR-join, AND-split, and AND-join.

Intuitively, an XOR-split gateway is a decision point: when the gateway is reached, one of the outgoing branches is activated (the mechanism for selection of a branch may be based on data conditions or probabilities). An AND-split gateway is a parallel branching point: when the gateway is reached, all its outgoing branches are activated. An XOR-join is a merge point: as soon as one of the incoming branches completes, the outgoing branch is activated. Finally, an AND-join is a synchronization point: when all incoming branches have completed, the outgoing branch is taken.

In this paper, we focus on *sound* workflow graphs that follow the same soundness properties as described for Petri nets in [9]. Based on this, the semantics of workflow graphs are defined similarly to that of Petri nets, as a token game. Given a workflow graph $W = (source, sink, N, F, c, l)$, a *marking* $M = \{f \mid f \in F\}$ of W is a set of active flows – i.e., having a token – that represents a state in the control-flow execution of the process. The *initial marking* of W is

²<https://www.bpmn.org/>

$source \bullet$, and the final marking $\bullet sink$. Given a marking M_1 , a node $n \in N$ of type “task” or “AND” can be executed – i.e., it is said to be *enabled* – iff $\bullet n \subseteq M_1$, and its execution produces the marking $M_2 = M_1 \setminus \bullet n \cup n \bullet$. In the same context, a node $n \in N$ of type “XOR” is enabled iff $M_1 \cap \bullet n \neq \emptyset$, and its execution produces the marking $M_2 = M_1 \setminus \bullet n \cup \{f_1\}$ such that $f_1 \in n \bullet$. Following the notation in [9], given a marking M_1 , we use $M_1 \xrightarrow{n} M_2$ to denote that n is enabled in M_1 , and its execution results in M_2 . We use $M_1 \xrightarrow{\sigma} M_2$ to denote that executing the sequence of nodes $\sigma = n_1, n_2, \dots, n_m$ from marking M_1 leads to marking M_2 . Finally, a marking M_2 is said to be a *reachable marking* from M_1 iff there exists a sequence (possibly empty) σ of nodes such that $M_1 \xrightarrow{\sigma} M_2$.

Table I depicts an example of workflow graph’s semantics through the replay of the trace (Register order, Check stock, Issue invoice, Register payment, Contact supplier, Pack and ship). Note that, in this example, the execution of XOR-splits generates the marking needed for the replay of this specific trace. However, according to the semantics described above, the paths involving other flows from XOR-split \bullet would also be valid.

Interpreting the markings of a workflow graph as its states, and the execution of nodes as transitions that move the execution from one state to another, one can build an automaton capturing the behavior of the workflow graph. This is the *reachability graph*.

Definition 2 (Reachability Graph). Given a workflow graph $W = (source, sink, N, F, c, l)$, a reachability graph of W is a directed graph $RG = (V, E, a)$ composed of a set $V \subseteq \mu$, being μ the set of all reachable markings of W , a set E of directed edges $e = (v_s, v_t)$ such that $v_s, v_t \in V$, and a mapping function $a : E \rightarrow N$ that maps each edge $e \in E$ with a node $n \in N$. For every edge $e = (v_s, v_t) \in E$, $v_s \xrightarrow{a(e)} v_t$, i.e., the execution of the node $a(e)$ in W , given the marking v_s , produces the marking v_t .

Given a workflow graph W , we define a reachability graph with V being a subset or all reachable markings of W . This implies that we allow for the existence of more than one reachability graph for W . For example, we call *complete reachability graph* to the reachability graph in which V corresponds to the set of all reachable markings of W , and such that the reachability graph supports any path in W from

$source$ to $sink$.

Definition 3 (Complete Reachability Graph). Given a workflow graph $W = (source, sink, N, F, c, l)$, a reachability graph $RG = (V, E, a)$ of W is a *complete reachability graph* of W iff $V = \mu$, and for any $M_1 \xrightarrow{n} M_2$ of W , there exists an edge $e = (v_s, v_t) \in E$ such that $a(e) = n$, $v_s = M_1$ and $v_t = M_2$.

However, as gateways play only a routing role – similar to silent transitions in Petri nets – it is sometimes desirable to exclude them from the reachability graph.

Definition 4 (Pure Reachability Graph). Given a workflow graph $W = (source, sink, N, F, c, l)$, a reachability graph $RG = (V, E, a)$ of W is a *pure reachability graph* iff 1) for any $M_i \in V$ and any $M_j \in \mu$ such that $M_i \xrightarrow{\sigma} M_j$ where $\exists! n \in \sigma \mid l(n) = \text{task}$, there exists an edge $e = (v_s, v_t) \in E$ such that $a(e) = n$, and $v_s = M_i$; and 2) for any $M_i \in V$ and any $M_j \in \mu$ such that $M_j \xrightarrow{\sigma} M_i$ where $\exists! n \in \sigma \mid l(n) = \text{task}$, there exists an edge $e = (v_s, v_t) \in E$ such that $a(e) = n$, and $v_t = M_i$. Therefore, for any path in W involving the execution of one single task and a (potentially empty) set of gateways, there is an edge in RG with the task-type node as label.

By abstracting the execution of gateways, one can navigate through the pure reachability graph based only on the sequence of executed activities (see Figure 2). This creates a design choice regarding when to traverse gateways: *i*) in an *eager* manner, i.e., as soon as they are enabled, or *ii*) in a *lazy* manner, only when it is strictly necessary to enable the activity that is going to be executed. Different gateway traversing policies yield different reachability graphs, all of them producing the same paths (of tasks).

Figure 2 shows a pure reachability graph of the workflow graph in Figure 1b following a lazy traversal policy. The execution of “Register order” advances the marking from $\{1\}$ to $\{2\}$. The AND-split gateway is only traversed when needed to execute either “Check stock” or “Issue invoice”, moving the marking from $\{2\}$ to either $\{3, 11\}$ or $\{4, 10\}$. The traversal policy w.r.t. AND gateways has a minor impact on the reachability graph, as it only replaces one marking with another, e.g., $\{2\}$ with $\{3, 10\}$. However, lazily traversing XOR-splits and eagerly traversing XOR-joins reduces the number of states in the reachability graph, while preserving

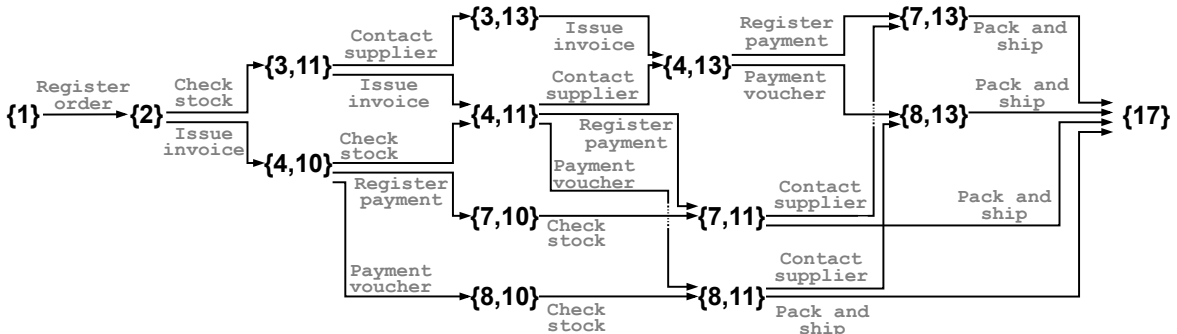


Figure 2. Pure reachability graph (lazy traversal policy) corresponding to the model in Figure 1b.

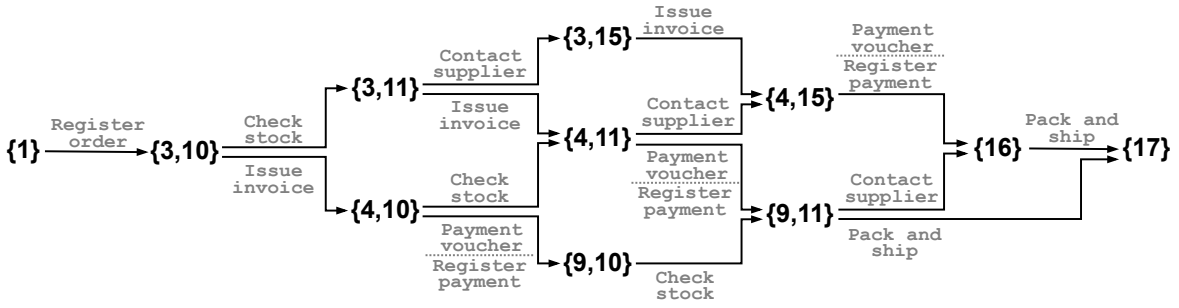


Figure 3. Pure reachability graph (lazy traversal policy only for XOR-splits) corresponding to the model in Figure 1b.

the behavior. For example, from state $\{3, 10\}$, the execution of “Issue invoice” leads to $\{4, 10\}$ with a lazy policy, but to both $\{5, 10\}$ and $\{6, 10\}$ with an eager policy. Similarly, from state $\{4, 10\}$, the executions of “Register payment” or “Payment voucher” lead to $\{9, 10\}$ with an eager policy, but to $\{7, 10\}$ and $\{8, 10\}$ with a lazy policy.

Figure 3 shows a pure reachability graph modeling the same behavior with fewer markings. Here, the traversal policy is lazy for XOR-splits but eager for other gateway types.

III. RELATED WORK

An intuitive and simple approach to compute the state of an ongoing case in a process model is to replay its trace prefix on the model, following the token game semantics sketched in Sec. II, and starting from the initial state – i.e., *source*. When the trace prefix does not fit the model, the (token-based) replay algorithm must apply heuristics that create and consume tokens to enable the execution of activities that are not enabled in the current state [6], [7]. In some situations, this artificial creation and/or consumption of tokens may map the trace prefix to an unreachable state. For example, given the process in Figure 1b, the unfitting trace prefix $\langle \text{Register order, Check stock, Contact supplier, Register payment} \rangle$, may correspond to one of two (reachable) scenarios: *i*) the ongoing marking $\{16\}$, where the invoice was issued but not registered due to an error in the system, thus, being the order ready to be packed and shipped; or *ii*), the ongoing marking $\{3, 15\}$, where the payment was wrongly registered due to the invoice not being generated, thus, the invoice still needs to be issued and the payment registered. Nevertheless, the artificial creation of tokens to enable the last activity in the trace prefix, “Register payment”, might generate the ongoing (unreachable) marking $\{3, 16\}$, which enables both the invoice issuing of the order and its packing and shipping.

Furthermore, the adjustments made by replay techniques may produce unreachable markings even in the case of fitting traces. For example, given the marking $\{5, 8\}$ for the process in Figure 1a, the execution of “Notify” may loop back through flow 12 and result in the marking $\{4, 8\}$, or loop back through flow 9 and produce the marking $\{5, 8\}$. In the context of fitting traces, only one of these decisions is correct, and it depends on the next executed activities. As replay algorithms make this decision locally, based solely on the previous activities, even fitting trace prefixes may lead to unreachable wrong markings.

The impact of unreachable markings for the purpose of log animation, although undesirable, may be considered acceptable. When the number of (artificially added) extra tokens in the animation is not high, they might be removed from the displayed animation once the trace is finished. However, they still present an issue that can cause misinterpretations during the analysis of the animation. Furthermore, unreachable markings are unsuitable for the purpose of short-term simulation. Starting the simulation of an ongoing case from an unreachable marking might result in the creation of unfitting traces, or even cause deadlocks that block the execution of the case.

A possible approach to handle non-fitting trace prefixes is to use prefix-alignment techniques [8], [11], [12] to align the prefix of the ongoing case with a prefix of the process model. Prefix-alignment techniques are designed to compute the minimum error correction needed to transform a trace prefix (of an ongoing case) into a trace prefix that can be produced by the process model. An error correction may be the skipping of an activity in the model that was not recorded in the case (move-on-model), or the skipping of an activity in the case that can not be executed in the model (move-on-log). Although prefix-alignment techniques are mainly designed for the purpose of conformance checking [13], the resulting alignment can then be used to replay the trace prefix on the process model and compute its current state. However, the problem of computing an optimal alignment has an exponential worst-case complexity. There have been several studies on efficiently computing trace alignments, but the resulting algorithms either only work for certain classes of process models, or they strike a tradeoff between computational complexity and optimality of the trace alignment [14]–[16].

Other approaches have researched the mapping of trace prefixes to abstract states of a process. For example, Burattin et al. represent in [17] the state of a trace prefix as a multiset of observed sequence patterns, among a set of frequent patterns in the log; while the work of Lee et al. [18] maps a trace prefix to a state in a Hidden Markov Model. Nevertheless, although these approaches allow us to estimate the fitness of a trace prefix w.r.t. a process model, they do not allow us to map a prefix to a state in the model.

To summarize, Table II compares the method proposed in this paper with token-based replay and prefix alignment approaches w.r.t. their ability to compute only reachable markings and their time complexity.

Table II
COMPARISON OF TECHNIQUES FOR STATE COMPUTATION.

| | Reachable markings | Time complexity | |
|--------------------|--------------------|--------------------|--------------------|
| | | Offline | Online |
| Token-based replay | | - | $\mathcal{O}(2^n)$ |
| Prefix-alignment | ✓ | - | $\mathcal{O}(2^n)$ |
| Our proposal | ✓ | $\mathcal{O}(2^n)$ | $\mathcal{O}(1)$ |

IV. N-GRAM INDEXING

Figure 4 depicts an overview of the approach proposed in this paper. In an offline phase, we compute a reachability graph of the process model (Sec. IV-A), which stores the possible states of a process case and how each activity displaces the execution from one state to another. Then, we construct an index that associates each n -gram (i.e., sequence of consecutive activity labels) with the state(s) in the process model it leads to (Sec. IV-B). Thus, the state of an ongoing case can be computed in constant time, at runtime, by searching in the index for the last n activities of the prefix (Sec. IV-C).

A. Reachability Graph Generation

The first step of our approach is to, given a process model, compute a (pure) reachability graph (see Def. 4) that models the behavior of the process as a state automaton. When performing this computation, we want to follow an eager traversing policy for join and AND-split gateways, while following a lazy policy for decision points, i.e., XOR-splits. One of the motivations for this lazy policy is to reduce the number of markings in the reachability graph (see Sec. II). In addition, when traversing a decision point, the selected path typically depends on execution data and/or on probabilities assigned to each path. For example, in the process in Figure 1b, the choice between flows 12 or 14 is not made arbitrarily, but based on whether the ordered products are in stock or not. In the context of log animation or short-term simulation, positioning the case in the state prior to a decision point allows the animation or simulation engine to select a branch based on branching probabilities or conditions, something that would not be possible if we returned a state after the decision point.

Alg. 1 presents the pseudocode of the algorithm to compute such reachability graph. The algorithm starts by advancing the initial marking until reaching decision points, tasks, or events (Alg. 1:1). The function `advLazy()` takes a marking and a workflow graph, and iteratively executes all enabled

AND/XOR-join and AND-split gateways, advancing the marking in the model until all enabled elements are either tasks, events, or decision points. This marking, which represents the initial marking of the process, is added as a vertex to the reachability graph (Alg. 1:2) and saved in the set of markings pending to explore (Alg. 1:4). Then, the markings that are pending to explore – i.e., the advanced initial markings and all markings that are added to the set in future iterations – are processed individually. This processing starts by advancing the current marking (M_c) through the enabled decision points, if any. Such advancement, performed by the function `advEager()`, produces a list of pairs $\langle n_i, M_i \rangle$ with a node of type task (n_i) that can be enabled by advancing through gateways from M_c , and the marking result of such advancement (M_i). Then, for each enabled node n_i and marking M_i , the algorithm replays the execution of n_i (Alg. 1:10), advances the resulting marking through AND/XOR-join and AND-split gateways (Alg. 1:11), saves the transition in the reachability graph (Alg. 1:12-15), and adds the marking to the queue of markings pending to explore (Alg. 1:16).

Importantly, the function `advEager()` does not trivially advance all branches until enabling each node n_i , but only the necessary branches to enable it. For example, following the model in Figure 1b, for $M_c = \{4, 11\}$, a full advancement produces four markings $\{5, 12\}$, $\{6, 12\}$, $\{5, 15\}$, and $\{6, 15\}$. Executing “Register payment” from both $\{5, 12\}$, and $\{5, 15\}$ would produce two markings in which the XOR-split enabled by flow 11 is already traversed. As previously reasoned in this section, the desired advanced marking in this case is $\{9, 11\}$. To avoid this, the function `advEager()` (Alg. 2) first advances by replaying the execution of all enabled gateways (Alg. 1:10,18-24). Then, when there are no more gateways enabled (Alg. 1:11), it goes over all enabled nodes and rollbacks the branches that were unnecessarily advanced to enable n_i . For example, after advancing $\{4, 11\}$ to $\{5, 12\}$, both “Register payment” and “Contact supplier” are enabled. For the pair where “Register payment” is n_i , the `rollback()` function rollbacks the flow 12 to 11, as its advancement was not required to enable n_i (producing $\{5, 11\}$). Similarly, for the pair where “Contact supplier” is n_i , the rollbacked marking corresponds to $\{4, 12\}$. For this, the function `rollback()` needs to advance, one by one, all combinations of enabled flows in the powerset $\mathbb{P}(M_c)$, until finding the smaller one needed for n_i to be enabled. Then, it rollbacks the remaining flows to their corresponding ones in the original marking (M').

The size of the reachability graph is exponential on the

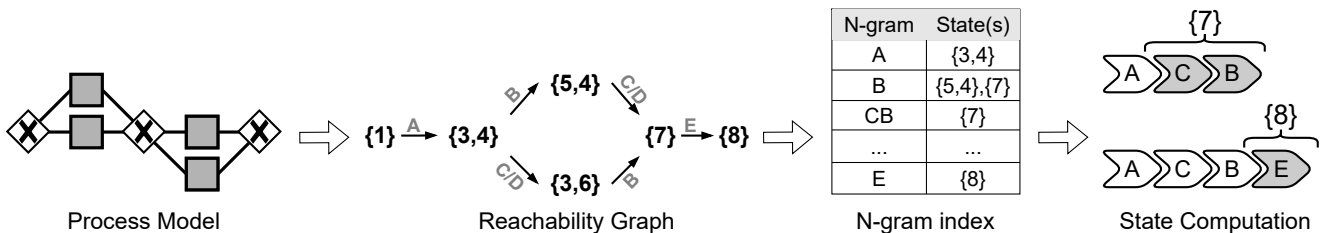


Figure 4. Overview of the approach proposed in this paper to compute the state of ongoing cases in constant time.

Algorithm 1: Compute a (pure) reachability graph.

Input: A Workflow graph
 $W = (source, sink, N, F, c, l)$.

Output: A (pure) reachability graph $RG = (V, E, a)$
of W (lazy traversing policy for decision points).

```

1  $M_1 \leftarrow \text{advLazy}(source, W)$ 
2  $V \leftarrow \{M_1\}$ 
3  $E \leftarrow \emptyset$ 
4  $M_{pend} \leftarrow \{M_1\}$ 
5  $M_{expl} \leftarrow \emptyset$ 
6 while  $M_{pend} \setminus M_{expl} \neq \emptyset$  do
7    $M_c \leftarrow M_i \mid M_i \in M_{pend} \setminus M_{expl}$ 
8    $M_{expl} \leftarrow M_{expl} \cup \{M_c\}$ 
9   for  $(n_i, M_i) \in \text{advEager}(M_c, W, \emptyset)$  do
10     $M_j \leftarrow \text{replay}(n_i, M_i, W)$ 
11     $M'_j \leftarrow \text{advLazy}(M_j, W)$ 
12     $V \leftarrow V \cup \{M'_j\}$ 
13     $e_j \leftarrow (M_c, M'_j)$ 
14     $E \leftarrow E \cup \{e_j\}$ 
15     $a(e_j) \leftarrow n_i$ 
16     $M_{pend} \leftarrow M_{pend} \cup \{M'_j\}$ 
17  end
18 end
19 return  $(V, E, a)$ 

```

number of activities in the model. Accordingly, the reachability graph computation has an exponential time complexity.

We presented the algorithm to compute a reachability graph over workflow graphs without inclusive (IOR) gateways. An extension to IOR gateways may be achieved by incorporating enablement and firing semantics of IOR gateways into the reachability graph computation algorithm, e.g., the semantics in [19]. We also foresee that the algorithm can be adapted to handle workflow nets [9]. In this context, a marking would correspond to a set of places in the net that hold a token, the token replay would follow the logic described in [9], a decision point would correspond to a place with more than one output transition, and the functions $\text{advLazy}()$ and $\text{advEager}()$ would advance through silent transitions instead of gateways.

B. N -gram Index Creation

Given the reachability graph computed in the previous stage, we build an index structure that maps each sequence of n consecutive activities (n -gram) that appear in any trace prefix of the model, to the marking(s) that this trace prefix leads to.

Definition 5 (N-gram index). Given a positive integer number $n \in \mathbb{N}^+$, the n -gram index of a pure reachability graph $RG = (V, E, a)$ is a list of key-value pairs ($key, value$) such that, for all $e_1 = (v_1, v_2), e_2 = (v_2, v_3), \dots, e_m = (v_m, v_{m+1}) \mid m \leq n$, and such that $e_1, e_2, \dots, e_m \in E$, there is an entry ($key, value$) such that $key = \langle a(e_1), a(e_2), \dots, a(e_m) \rangle$ and $v_{m+1} \in value$, i.e., for all sequences of n or less consecutive edges in RG , the target marking of the last edge is part of the value associated to the sequence formed by the edges' labels.

Algorithm 2: Advance a marking through gateways.

Input: A marking M , a workflow graph
 $W = (so, si, N, F, c, l)$, and a set of explored markings M_{expl} .

Output: A list of pairs (n_i, M_i) where n_i is a node of type task and M_i is the marking that enables n_i .

```

1 Function  $\text{advEager}(M, W, M_{expl})$ 
2    $P \leftarrow \emptyset$ 
3    $M' \leftarrow \text{advLazy}(M, W)$ 
4    $M_{pend} \leftarrow \{M'\}$ 
5   while  $M_{pend} \neq \emptyset$  do
6      $M_{fut} \leftarrow \emptyset$ 
7     for  $M_c \in M_{pend}$  do
8       if  $M_c \notin M_{expl}$  then
9          $M_{expl} \leftarrow M_{expl} \cup \{M_c\}$ 
10         $G \leftarrow \{n_i \in N \mid l(n_i) \in \{AND, XOR\} \wedge \text{isEnabled}(n_i, M_c, W)\}$ 
11        if  $G = \emptyset$  then
12           $N_{enab} \leftarrow \{n_i \in N \mid l(n_i) = \text{task} \wedge \text{isEnabled}(n_i, M_c, W)\}$ 
13          for  $n_i \in N_{enab}$  do
14             $M_r \leftarrow \text{rollbk}(M_c, M', n_i, W)$ 
15             $P \leftarrow P \cup \{(n_i, M_r)\}$ 
16          end
17        else
18           $g_c \leftarrow g_i \mid g_i \in G$ 
19          if  $l(g_c) = AND \wedge |g_c \bullet| > 1$  then
20             $P \leftarrow P \cup \text{advEager}(M_c, W, M_{expl})$ 
21          else
22             $M_{adv} \leftarrow \text{replay}(g_c, M_c, W)$ 
23             $M_{fut} \leftarrow M_{fut} \cup M_{adv}$ 
24          end
25        end
26      end
27    end
28     $M_{pend} \leftarrow M_{fut}$ 
29  end
30  return  $P$ 

```

It must be noted that the n -gram index behaves as a monotonic function when the n -gram grows backward. For example, in Figure 3, the 1-gram (Issue invoice) leads to states $\{4, 10\}$, $\{4, 11\}$, and $\{4, 15\}$. Any 2-gram ending in “Issue invoice” must lead to a subset of those markings. Thus, when building the n -gram index, the expansion can be pruned when a growing m -gram gives a deterministic solution.

Table III depicts the n -gram index (for $n = 3$) corresponding to the reachability graph in Figure 3. As the 1-gram (Pack and ship) leads to one single state (deterministic), it is unnecessary to store any 2-gram with “Pack and ship” as its last activity. Conversely, the 1-gram (Contact supplier) leads to 3 different markings and, thus, it is expanded until all the

Table III
3-GRAM INDEX OF THE REACHABILITY GRAPH IN FIGURE 3.

| n -gram | State(s) |
|---|---------------------------|
| ⟨ Register order ⟩ | {3, 10} |
| ⟨ Check stock ⟩ | {3, 11}, {4, 11}, {9, 11} |
| ⟨ Issue invoice ⟩ | {4, 10}, {4, 11}, {4, 15} |
| ⟨ Contact supplier ⟩ | {3, 15}, {4, 15}, {16} |
| ⟨ Payment voucher ⟩ | {9, 10}, {9, 11}, {16} |
| ⟨ Register payment ⟩ | {9, 10}, {9, 11}, {16} |
| ⟨ Pack and ship ⟩ | {17} |
| ⟨ Register order, Check stock ⟩ | {3, 11} |
| ⟨ Issue invoice, Check stock ⟩ | {4, 11}, |
| ⟨ Payment voucher, Check stock ⟩ | {9, 11} |
| ⟨ Register payment, Check stock ⟩ | {9, 11} |
| ⟨ Register order, Issue invoice ⟩ | {4, 10} |
| ⟨ Check stock, Issue invoice ⟩ | {4, 11} |
| ⟨ Contact supplier, Issue invoice ⟩ | {4, 15} |
| ⟨ Check stock, Contact supplier ⟩ | {3, 15}, {4, 15}, {16} |
| ⟨ Issue invoice, Contact supplier ⟩ | {4, 15} |
| ⟨ Payment voucher, Contact supplier ⟩ | {16} |
| ⟨ Register payment, Contact supplier ⟩ | {16} |
| ⟨ Issue invoice, Payment voucher ⟩ | {9, 10}, {9, 11}, {16} |
| ⟨ Check stock, Payment voucher ⟩ | {9, 11} |
| ⟨ Contact supplier, Payment voucher ⟩ | {16} |
| ⟨ Issue invoice, Register payment ⟩ | {9, 10}, {9, 11}, {16} |
| ⟨ Check stock, Register payment ⟩ | {9, 11} |
| ⟨ Contact supplier, Register payment ⟩ | {16} |
| ⟨ Register order, Check stock, Contact supplier ⟩ | {3, 15} |
| ⟨ Issue invoice, Check stock, Contact supplier ⟩ | {4, 15} |
| ⟨ Payment voucher, Check stock, Contact supplier ⟩ | {16} |
| ⟨ Register payment, Check stock, Contact supplier ⟩ | {16} |
| ⟨ Register order, Issue invoice, Payment voucher ⟩ | {9, 10} |
| ⟨ Check stock, Issue invoice, Payment voucher ⟩ | {9, 11} |
| ⟨ Contact supplier, Issue invoice, Payment voucher ⟩ | {16} |
| ⟨ Register order, Issue invoice, Register payment ⟩ | {9, 10} |
| ⟨ Check stock, Issue invoice, Register payment ⟩ | {9, 11} |
| ⟨ Contact supplier, Issue invoice, Register payment ⟩ | {16} |

resulting n -grams are deterministic, or $n = 3$ (the maximum size for this example).

Given the monotonicity of the n -gram index, there exist (pure) reachability graphs – and, by extension, workflow graphs – for which the n -gram index would never need to grow the prefixes more than a certain m , $m < n$. For example, given the reachability graph in Figure 3, the 3-gram is enough to identify any ongoing state. We call this the K -complexity of a workflow graph, and it corresponds to the maximum n -gram size needed to unambiguously identify the ongoing state of a fitting case. The K -complexity of a sequential workflow graph is clearly $K = 1$. However, when a p -branch parallel structure is present, the K -complexity of the model equals to the sum of the lengths of the $p - 1$ longest branches, plus one. In this context, the length of a branch is equal to the number of activities of its longest sequence. Finally, one can trivially see that the K -complexity of a workflow graph is infinite if there is a loop in a parallel branch.

C. Online State Computation

Given a trace prefix t , we call its last m consecutive activities the *ending m -gram* of t . To compute the state of a trace prefix t , we search the index for each of its ending m -grams ($m < n$). Assuming t contains only activities observed in the log from which the index was built (no previously unseen activities) we will always find a match, since the ending 1-gram (a single activity) is a 1-gram of the log and hence included in the index. We retain the matching index entry with the smallest m that is associated with one single state (no ambiguity) or else the index entry with the smallest number of associated states (the least ambiguous). In the latter scenario, we randomly select one of the states. If implemented as a hash table, the complexity of this online step is $O(1)$ amortized.

Following with the example in Table III, and given the trace ⟨Register order, Issue invoice, Check stock, Contact supplier⟩, the first search would be for the 1-gram ⟨Contact supplier⟩. As the result of this search is a set of three states, the search would continue with the 2-gram ⟨Check stock, Contact supplier⟩, which also returns a set of three states. Finally, the search would grow the n -gram to ⟨Issue invoice, Check stock, Contact supplier⟩, which returns the state {4, 15} as a result. Thus, when resuming the simulation of this ongoing case, a token would be placed in flows 4 and 15 of Figure 1b, which enables the execution of “Register payment” and “Payment voucher”.

V. EVALUATION

This section reports on an experimental evaluation of: *i*) the ability of the proposed approach to accurately compute already-known states of ongoing cases, *ii*) its accuracy in real-life scenarios where the state of the process is unknown, and *iii*) its efficiency. The first part of the evaluation addresses the following question:

Evaluation Question 1 (EQ1): *is the proposed approach able to accurately compute the already-known state of an ongoing case?*

To assess this, we designed a set of simulation scenarios where the state at each step of a process case is known. The designed processes cover different levels of complexity. We applied different levels of noise to the designed scenarios in order to study the impact of possible deviations from the expected behavior, as well as of wrongly recorded data.

The second part of the evaluation addresses the accuracy on real-life processes, where cases often deviate from the expected behavior and the actual state of a case unknown. This part addresses the following question:

Evaluation Question 2 (EQ2): *given an ongoing case, where the state is unknown, is the proposed approach able to compute a future-equivalent state?*

The state of an ongoing case in real-life processes is typically unknown, as the only available information are the recorded activity instances and their attributes. Thus, we seek to compute future-equivalent states, where two states are future-equivalent if they allow for the execution of the same remaining behavior.

This part of the evaluation is also designed to validate the efficiency of the proposed approach in real-life scenarios, by addressing the following question:

Evaluation Question 3 (EQ3): *is the approach able to handle thousands of traces per second?*

A. Synthetic Evaluation

This section describes the evaluation performed to validate the accuracy of the proposal when estimating the already-known state of ongoing cases of a process (EQ1). We split this evaluation question into two parts. The first part (EQ1.1) analyzes the accuracy of the proposal for a variety of scenarios with different (K -)complexities. The second part (EQ1.2) focuses on the impact that nondeterministic scenarios – where a fitting trace may lead to multiple states, and the correct one depends on the next executed activities (see Sec. I) – may have on the accuracy of the technique.

Datasets & Setup. To evaluate EQ1.2, we designed five simulation process models with different complexities. One sequential process with two decision points (“Seq”), and one variant of this process with loops (“Loop”). Both processes present a K -complexity (see Sec. IV-B) of one, meaning that, in a perfect-fit case, the last executed activity is enough to denote the ongoing state. In addition, three more processes containing parallel structures of two (“K3”), three (“K5”), and five (“K10”) concurrent branches with a K -complexity of three, five, and ten, respectively. Regarding EQ1.2, we used the process model depicted in Figure 1a. We generated a simulated log of 1000 cases for each of these models, and retained the first m recorded activities of each case to represent ongoing cases. For each case, m is a random number between three (minimum required size for the noise injection commented below) and the number of events recorded in that case. Finally, for each event log (“Raw”), we injected three levels of noise by randomly applying, to each ongoing case, one (“Noise-1”), two (“Noise-2”), and three (“Noise-3”) operations from *i*) adding a new event of a random activity at a random position, *ii*) deleting a random event, or *iii*) swapping the order of two random consecutive events.

As a baseline, we used the token-based replay approach presented in [7]. This approach (*TokenR*) follows the token-replay semantics described in Sec. II. In non-conforming situations, where the next recorded activity is not enabled given the current marking, the replay algorithm applies a set of heuristics to artificially add tokens in order to enable it.³ As commented in Sec. III, token-replay techniques might produce unreachable states in unfitting situations. For this reason, we considered an approach based on prefix-alignments [8] as a second baseline (*PrefAl*). We used the prefix-alignment proposal presented in [8] in order to obtain a fitting alignment of each ongoing case. Then, we replayed it in the reachability graph computed by our proposal to obtain the corresponding (reachable) state. We selected the approach proposed in [8],

³We used the latest implementation available in PM4PY [20], a well-known Python library providing a varied set of tools for process mining.

Table IV
RATIO OF ONGOING STATES CORRECTLY ESTIMATED BY THE EVALUATED TECHNIQUES FOR THE SYNTHETIC DATASETS. THE SHADOWED CELLS DENOTE, FOR EACH DATASET, THE BEST RESULT (± 0.01).

| | | Seq | Loop | K3 | K5 | K10 | Kamb |
|---------|---------------|------|------|------|------|------|------|
| Raw | <i>TokenR</i> | 1.00 | 1.00 | 1.00 | 1.00 | 1.00 | 0.98 |
| | <i>PrefAl</i> | 1.00 | 1.00 | 1.00 | 1.00 | 1.00 | 1.00 |
| | 3-gram | 1.00 | 1.00 | 1.00 | 0.98 | 0.51 | 0.98 |
| | 5-gram | 1.00 | 1.00 | 1.00 | 1.00 | 0.89 | 1.00 |
| | 10-gram | 1.00 | 1.00 | 1.00 | 1.00 | 1.00 | 1.00 |
| Noise-1 | <i>TokenR</i> | 0.05 | 0.04 | 0.15 | 0.29 | 0.37 | 0.38 |
| | <i>PrefAl</i> | 0.75 | 0.74 | 0.76 | 0.78 | 0.69 | 0.69 |
| | 3-gram | 0.82 | 0.81 | 0.80 | 0.72 | 0.36 | 0.69 |
| | 5-gram | 0.82 | 0.81 | 0.80 | 0.72 | 0.58 | 0.70 |
| | 10-gram | 0.82 | 0.81 | 0.80 | 0.72 | 0.63 | 0.71 |
| Noise-2 | <i>TokenR</i> | 0.04 | 0.04 | 0.04 | 0.11 | 0.12 | 0.26 |
| | <i>PrefAl</i> | 0.57 | 0.57 | 0.62 | 0.63 | 0.53 | 0.58 |
| | 3-gram | 0.64 | 0.66 | 0.63 | 0.58 | 0.31 | 0.60 |
| | 5-gram | 0.64 | 0.66 | 0.63 | 0.58 | 0.45 | 0.61 |
| | 10-gram | 0.64 | 0.66 | 0.63 | 0.58 | 0.47 | 0.61 |
| Noise-3 | <i>TokenR</i> | 0.00 | 0.01 | 0.01 | 0.04 | 0.05 | 0.16 |
| | <i>PrefAl</i> | 0.44 | 0.43 | 0.50 | 0.54 | 0.40 | 0.48 |
| | 3-gram | 0.51 | 0.55 | 0.49 | 0.50 | 0.27 | 0.49 |
| | 5-gram | 0.51 | 0.55 | 0.49 | 0.51 | 0.37 | 0.49 |
| | 10-gram | 0.51 | 0.55 | 0.49 | 0.51 | 0.39 | 0.49 |

as it includes a prefix-catching strategy to avoid recalculating prefix-alignments for event sequences that were already observed in the past, thus reducing computational time.

Results & Discussion. Table IV depicts, for each dataset, the percentage of ongoing cases in which the evaluated techniques computed the correct state. Regarding EQ1.1, evaluated through “Seq”, “Loop”, “K3”, “K5”, and “K10”, both *TokenR* and *PrefAl* obtain an accuracy of 100% in the “Raw” datasets, as the absence of noise ensures a perfect replay of the trace prefixes. For the same reason, the n -gram index proposals obtain an accuracy of 100% in the processes with a K -complexity lower or equal to each n . As commented in Sec. IV-B, in fitting traces, the last K executed activities are enough to denote the ongoing state of a case.

In the datasets with noise, as expected, the accuracy of all techniques decreases as the noise level increases. However, it does not affect all proposals in the same way. *TokenR* presents the higher impact, obtaining the lowest accuracy. This is due to the artificial addition of tokens in unfitting scenarios, which results in unreachable markings. Regarding the other techniques, in the processes with K -complexity of 1, the noise has a stronger (negative) impact in *PrefAl*, leading to our proposal to present better accuracy in all datasets.⁴ However, this ranking is inverted as the K -complexity of the process increases. The reasoning behind this phenomenon comes from the fact that the n -gram index proposal estimates the ongoing state based on, at most, the last n executed activities, while *PrefAl* uses the entire ongoing case to find the best alignment. The smaller the K -complexity of the process – thus, the

⁴The performance of the evaluated n -gram index proposals is similar in “Seq”, “Loop”, and “K3” because, as the K -complexity of these models is lower or equal to 3, an index with $n = 3$ is already complete. Similarly, 5-gram and 10-gram proposals present identical performance in “K5”.

Table V
CHARACTERISTIC OF THE (PROCESSED) REAL-LIFE EVENT LOGS AND ONGOING CASES USED IN THE EVALUATION OF RQ2 AND RQ3.

| | # Cases | # Events | # Activities | Trace length | | | Ongoing cases length | | |
|-----------------------|---------|-----------|--------------|--------------|--------|-------|----------------------|--------|-------|
| | | | | Min | Median | Max | Min | Median | Max |
| BPIC12 | 13,087 | 164,506 | 23 | 3 | 7 | 96 | 1 | 3 | 81 |
| BPIC13 _{inc} | 7,554 | 65,533 | 4 | 1 | 6 | 123 | 1 | 3 | 110 |
| BPIC14 | 46,616 | 466,737 | 39 | 1 | 7 | 178 | 1 | 3 | 167 |
| BPIC17 | 31,509 | 582,374 | 24 | 8 | 18 | 62 | 1 | 8 | 54 |
| BPIC18 | 43,809 | 2,514,266 | 41 | 24 | 49 | 2,973 | 1 | 26 | 1,579 |
| BPIC19 | 251,734 | 1,595,923 | 42 | 1 | 5 | 990 | 1 | 2 | 663 |
| BPIC20 _{dom} | 10,500 | 56,437 | 17 | 1 | 5 | 24 | 1 | 3 | 13 |
| BPIC20 _{int} | 6,449 | 72,151 | 34 | 3 | 10 | 27 | 1 | 5 | 23 |
| BPIC20 _{pre} | 2,099 | 18,246 | 29 | 1 | 8 | 21 | 1 | 4 | 17 |
| BPIC20 _{req} | 6,886 | 36,796 | 19 | 1 | 5 | 20 | 1 | 2 | 13 |
| BPIC20 _{tra} | 7,065 | 86,581 | 51 | 3 | 11 | 90 | 1 | 5 | 44 |
| Sepsis | 1,050 | 15,214 | 16 | 3 | 13 | 185 | 1 | 6 | 85 |

Table VI
FITNESS OF THE DISCOVERED PROCESS MODELS.

| | IMf ₁₀ | | IMf ₂₀ | | IMf ₅₀ | |
|-----------------------|-------------------|--------------|-------------------|--------------|-------------------|--------------|
| | Fitness | # AND-splits | Fitness | # AND-splits | Fitness | # AND-splits |
| BPIC12 | 0.94 | 5 | 0.94 | 2 | 0.80 | 3 |
| BPIC13 _{inc} | 0.99 | 1 | 0.96 | 1 | 0.78 | 1 |
| BPIC14 | - | 6 | 0.98 | 1 | 0.99 | 0 |
| BPIC17 | 0.99 | 0 | 0.93 | 2 | 0.76 | 2 |
| BPIC18 | - | 5 | - | 5 | - | 2 |
| BPIC19 | - | 4 | - | 5 | - | 6 |
| BPIC20 _{dom} | 0.95 | 0 | 0.94 | 0 | 0.94 | 0 |
| BPIC20 _{int} | 0.95 | 3 | 0.89 | 2 | 0.85 | 0 |
| BPIC20 _{pre} | 0.94 | 5 | 0.88 | 4 | 0.81 | 1 |
| BPIC20 _{req} | 0.96 | 3 | 0.92 | 1 | 0.92 | 1 |
| BPIC20 _{tra} | - | 6 | 0.76 | 6 | 0.67 | 5 |
| Sepsis | 0.98 | 2 | 0.96 | 2 | 0.86 | 2 |

smaller the n needed –, the lower the probability of potential noise affecting the n -gram index proposal. At the same time, when affecting both techniques, the noise has a lower impact in *PrefAl*. This is due to our proposal performing an exact matching for the n -gram prefix, while *PrefAl* allowing for deviations when aligning the ongoing case with the model.

Regarding EQ1.2, the results of “Kamb” in Table IV for the datasets without noise (i.e., fitting ongoing cases) show how *TokenR* fails to compute the ongoing state in some situations. This error corresponds to the drawback of this approach described in Sec. III. When the replay reaches a point in which there exist multiple distinct token movements to enable the next recorded activity instance, *TokenR* has to decide which of them to replay. When the followed path is incorrect, the following activity instance may not be enabled, causing the repair heuristics to create unreachable markings even for fitting traces. *PrefAl* obtains an accuracy of 100% in these datasets due to its perfect alignment of fitting traces. As alignment techniques save a search space with multiple possible paths, they never discard a path with no deviations. Regarding the n -gram index proposals, even though the theoretical K -complexity of the model (see Figure 1a) is infinite, the probability of needing more than 5 consecutive activities to denote the ongoing state is really low. For this reason, 5-gram and 10-gram also present a perfect accuracy. Finally, with respect to the impact of noise, the results show a similar

trend to that of deterministic logs, where all techniques see their accuracy reduced as the noise increases.

In conclusion, for fitting traces, *PrefAl* always computes the correct state. As expected, the n -gram index approach fails when $n \leq$ the K -complexity of the model. Meanwhile, the *TokenR* approach fails when there are multiple token movements to enable the next recorded activity instance.

In the presence of noise, the n -gram approach achieves higher accuracy for models with low K -complexity. However, when the K -complexity of the model increases, it underperforms the *PrefAl*. This result is expected. When the K -complexity is high, the n -gram approach does not have sufficient information to compute the correct state. The presence of noise aggravates this lack of information. Meanwhile, when the K -complexity is low, the n -gram approach has sufficient information to compute the correct state, while being less likely to be affected by the noise since it only looks at the last n events in the prefix. The *PrefAl* is more likely to be affected by noise, since it looks at the whole prefix. Prefix alignment techniques are designed to find a minimal set of “skip event” (move-on-log) or “add event” (move-on-model) operations to transform a given trace prefix into a prefix that can be parsed by a process model. In the presence of noise, these techniques find an alignment containing a minimal set of operations to correct this noise, but when this alignment is replayed against the model, the replay may or may not lead to

the state that would be reached had the noise not been present.

Meanwhile, in the presence of noise, the *TokenR* approach often returns unreachable states. The results suggest that *TokenR* is not a suitable approach for state computation when the input trace prefixes do not fit the behavior of the model.

B. Real-life Evaluation

This section describes the accuracy evaluation performed on real-life scenarios (EQ2), as well as the evaluation of the efficiency of our proposal (EQ3).

Datasets & Setup. We selected 12 real-life event logs from the publicly available collection at the 4TU Centre for Research Data ⁵ corresponding to business processes, as opposed to, e.g., software development processes. We discarded the logs of the Business Process Intelligence Challenges (BPIC) of 2011 and 2015, as the high number of activities (over 300) and low variant frequency prevented all approaches from retrieving a result in a reasonable time. We also discarded the Road Traffic Fines and BPIC 2013 (closed and open problems) due to having an average case length below 4, which would lead to most ongoing cases having only 1 or 2 events. The remaining selected logs correspond to the BPIC of 2012, 2013 (incidents), 2014, 2017, 2018, 2019, and 2020, and a Sepsis patient treatment process. We preprocessed the logs with lifecycle information by retaining only the events corresponding to the activity completion, i.e., complete, closed, etc. Then, we obtained the ongoing cases by retaining the first m recorded activities of each complete case, being m a random number between one and the number of events recorded in each case minus one. Table V depicts the characteristics of these preprocessed logs, containing from 4 to 51 activities and from 15,000 to 2,500,000 events. Regarding the ongoing cases, their minimum length is 1, their median ranges from 2 to 26, and their maximum from 13 to 1,579.

For each log, we used the Inductive Miner infrequent [21] to discover a workflow graph. To analyze how the accuracy varies depending on the fitness, we discovered three process models (with thresholds of 10%, 20%, and 50%) per log. Table VI depicts the characteristics of the discovered models. The fitness ranges from 0.94 to 0.99 (10% threshold), from 0.88 to 0.98 (20% threshold), and from 0.67 to 0.99 (50% threshold). Six out of the 36 models are perfectly sequential, while the rest contain from 1 to 6 AND-split gateways.

Due to the high tendency of *TokenR* to create unreachable markings with additional tokens (see evaluation of EQ1), we discarded this approach for the evaluation of EQ2 and EQ3. Accordingly, this evaluation compares the performance and efficiency of *PrefixAl* and multiple versions of our proposal.

Due to the lack of ground truth in the case of real-life processes, as the state of each ongoing case is unknown, the evaluation of EQ2 cannot be performed similarly to that of EQ1. For this reason, as a measure of goodness to assess if the computed state is “future-equivalent” w.r.t. the (unknown)

Table VII
ACCURACY ON REAL-LIFE LOGS (RATIO OF ONGOING CASES FOR WHICH THE NEXT RECORDED ACTIVITY IS ENABLED IN THE COMPUTED STATE).
SHADOWED CELLS ARE BEST RESULT FOR EACH DATASET (± 0.01).

| | <i>PrefAl</i> | 3-gram | 4-gram | 5-gram | |
|-------------------|-----------------------|--------|--------|--------|------|
| IMf ₁₀ | BPIC12 | 0.96 | 0.96 | 0.96 | 0.97 |
| | BPIC13 _{inc} | 0.99 | 0.99 | 0.99 | 0.99 |
| | BPIC14 | - | 0.93 | 0.93 | 0.93 |
| | BPIC17 | 0.98 | 0.99 | 0.99 | 0.99 |
| | BPIC18 | - | - | - | - |
| | BPIC19 | - | 0.98 | 0.98 | - |
| | BPIC20 _{dom} | 0.93 | 0.94 | 0.94 | 0.94 |
| | BPIC20 _{int} | 0.92 | 0.94 | 0.94 | 0.94 |
| | BPIC20 _{pre} | 0.91 | 0.93 | 0.93 | 0.93 |
| | BPIC20 _{req} | 0.95 | 0.96 | 0.96 | 0.96 |
| | BPIC20 _{tra} | - | 0.83 | 0.79 | 0.85 |
| | Sepsis | 0.86 | 0.81 | 0.76 | 0.76 |
| IMf ₂₀ | BPIC12 | 0.96 | 0.96 | 0.96 | 0.96 |
| | BPIC13 _{inc} | 0.78 | 0.79 | 0.81 | 0.81 |
| | BPIC14 | 0.97 | 0.97 | 0.97 | 0.97 |
| | BPIC17 | 0.93 | 0.91 | 0.91 | 0.91 |
| | BPIC18 | - | 0.88 | 0.89 | 0.89 |
| | BPIC19 | - | 0.91 | 0.91 | - |
| | BPIC20 _{dom} | 0.82 | 0.89 | 0.89 | 0.89 |
| | BPIC20 _{int} | 0.80 | 0.86 | 0.86 | 0.86 |
| | BPIC20 _{pre} | 0.76 | 0.81 | 0.81 | 0.81 |
| | BPIC20 _{req} | 0.83 | 0.89 | 0.89 | 0.89 |
| | BPIC20 _{tra} | 0.61 | 0.73 | 0.73 | 0.73 |
| | Sepsis | 0.99 | 0.76 | 0.79 | 0.79 |
| IMf ₅₀ | BPIC12 | 0.59 | 0.61 | 0.61 | 0.61 |
| | BPIC13 _{inc} | 0.62 | 0.73 | 0.73 | 0.73 |
| | BPIC14 | 1.00 | 1.00 | 1.00 | 1.00 |
| | BPIC17 | 0.68 | 0.72 | 0.72 | 0.72 |
| | BPIC18 | - | 0.84 | 0.84 | 0.84 |
| | BPIC19 | - | 0.55 | 0.64 | 0.66 |
| | BPIC20 _{dom} | 0.82 | 0.89 | 0.89 | 0.89 |
| | BPIC20 _{int} | 0.77 | 0.86 | 0.86 | 0.86 |
| | BPIC20 _{pre} | 0.75 | 0.85 | 0.85 | 0.85 |
| | BPIC20 _{req} | 0.83 | 0.89 | 0.89 | 0.89 |
| | BPIC20 _{tra} | 0.60 | 0.65 | 0.65 | 0.65 |
| | Sepsis | 0.91 | 0.63 | 0.64 | 0.66 |

real state, we report on whether the state enables the next activity recorded in the ongoing case.⁶

Results & Discussion. Regarding EQ2, Table VII shows the accuracy of the evaluated methods. The n -gram index yields higher accuracy than the *PrefAl* technique in most cases. Although the differences are negligible in the models with higher complexity (IMf₁₀), they grow as the support of the model decreases. Furthermore, in 7 out of the 36 scenarios, *PrefAl* was not able to compute the state of ongoing cases in a reasonable time, while the n -gram index method did. The Sepsis Cases dataset is an exception, where *PrefAl* outperforms the n -gram index method. As expected, the accuracy of the techniques generally decreases with the support.

Regarding EQ3, Figure VIII shows the runtimes of each proposal. *PrefAl* reuses pre-computed heuristics to reduce the space explored by the A^* which, in logs with tens of thousands of cases, reduces the average runtime of the first

⁶Given that we measure the goodness of the computed state based on whether it enables the next observed activity, one may suggest that any technique that predicts the next activity in a case is a possible baseline in this evaluation. However, we note that an approach that predicts the next activity (e.g. using a deep learning technique), is not a suitable baseline because it does not return a state (i.e. a marking) in the process model.

⁵<https://data.4tu.nl/>

Table VIII

RUNTIMES ON THE REAL-LIFE LOGS (IN SECONDS NEEDED TO HANDLE ONE ONGOING CASE). THE SHADOWED CELLS DENOTE THE LOWEST RUNTIMES PER DATASET (± 0.01). INDEX CONSTRUCTION TIMES ARE ALSO INCLUDED.

| | <i>PrefAl</i> | N-gram index | | | | | | | |
|-------------------|-----------------------|--------------------|----------|--------|--------|--------|--------|----------|------|
| | | Reachability Graph | 3-gram | | 4-gram | | 5-gram | | |
| | | | Avg | Index | Avg | Index | Avg | Index | Avg |
| IMf ₁₀ | BPIC12 | 0.50 | 0.35 | 0.02 | 4e-6 | 0.07 | 4e-6 | 0.27 | 3e-6 |
| | BPIC13 _{inc} | 0.17 | 0.01 | 0.01 | 8e-6 | 0.01 | 3e-6 | 0.01 | 5e-6 |
| | BPIC14 | - | 35.92 | 8.29 | 5e-6 | 180.08 | 3e-6 | 5,588.70 | 5e-5 |
| | BPIC17 | 0.10 | 0.01 | 0.01 | 2e-6 | 0.01 | 2e-6 | 0.01 | 3e-6 |
| | BPIC18 | - | - | - | - | - | - | - | - |
| | BPIC19 | - | 32.44 | 2.50 | 2e-5 | 79.12 | 1e-5 | - | - |
| | BPIC20 _{dom} | 0.03 | 0.01 | 0.01 | 2e-6 | 0.01 | 1e-6 | 0.01 | 2e-6 |
| | BPIC20 _{int} | 0.25 | 0.13 | 0.01 | 2e-6 | 0.01 | 3e-6 | 0.03 | 4e-6 |
| | BPIC20 _{pre} | 0.39 | 0.16 | 0.01 | 7e-6 | 0.01 | 1e-7 | 0.02 | 5e-6 |
| | BPIC20 _{req} | 0.16 | 0.02 | 0.01 | 2e-6 | 0.01 | 2e-6 | 0.01 | 3e-6 |
| | BPIC20 _{tra} | - | 1,102.26 | 112.60 | 2e-4 | 580.47 | 2e-4 | 3,475.74 | 3e-4 |
| Sepsis | 0.42 | 6.85 | 0.33 | 1e-5 | 2.09 | 1e-5 | 13.47 | 3e-5 | |
| IMf ₂₀ | BPIC12 | 0.31 | 0.09 | 0.01 | 2e-6 | 0.02 | 2e-6 | 0.02 | 3e-6 |
| | BPIC13 _{inc} | 0.14 | 0.01 | 0.01 | 4e-6 | 0.01 | 3e-6 | 0.01 | 6e-6 |
| | BPIC14 | 0.78 | 0.01 | 0.01 | 2e-6 | 0.01 | 3e-6 | 0.01 | 3e-6 |
| | BPIC17 | 0.48 | 0.31 | 0.02 | 4e-6 | 0.04 | 5e-6 | 0.13 | 8e-6 |
| | BPIC18 | - | 13.98 | 0.19 | 2e-5 | 1.46 | 2e-5 | 11.00 | 2e-5 |
| | BPIC19 | - | 254.50 | 23.53 | 5e-5 | 423.70 | 5e-5 | - | - |
| | BPIC20 _{dom} | 0.02 | 0.01 | 0.01 | 1e-6 | 0.01 | 2e-6 | 0.01 | 5e-7 |
| | BPIC20 _{int} | 0.18 | 0.06 | 0.06 | 4e-6 | 0.06 | 2e-6 | 0.06 | 5e-6 |
| | BPIC20 _{pre} | 0.19 | 0.15 | 0.01 | 1e-7 | 0.02 | 1e-7 | 0.06 | 1e-7 |
| | BPIC20 _{req} | 0.02 | 0.01 | 0.01 | 4e-6 | 0.01 | 6e-6 | 0.01 | 4e-6 |
| | BPIC20 _{tra} | 3.02 | 2.81 | 0.61 | 5e-6 | 10.14 | 4e-6 | 176.56 | 5e-6 |
| Sepsis | 0.32 | 11.17 | 0.38 | 1e-5 | 2.02 | 2e-5 | 9.91 | 4e-5 | |
| IMf ₅₀ | BPIC12 | 0.16 | 0.02 | 0.01 | 3e-6 | 0.01 | 6e-6 | 0.01 | 5e-6 |
| | BPIC13 _{inc} | 0.14 | 0.01 | 0.01 | 3e-6 | 0.01 | 4e-6 | 0.01 | 4e-6 |
| | BPIC14 | 1.21 | 0.15 | 0.01 | 4e-6 | 0.01 | 3e-6 | 0.01 | 3e-6 |
| | BPIC17 | 0.40 | 0.15 | 0.01 | 5e-6 | 0.02 | 3e-6 | 0.08 | 5e-6 |
| | BPIC18 | - | 8.18 | 1.42 | 2e-5 | 33.31 | 2e-5 | 793.41 | 1e-5 |
| | BPIC19 | - | 31.72 | 9.92 | 2e-5 | 202.82 | 3e-5 | 5,639.26 | 3e-5 |
| | BPIC20 _{dom} | 0.02 | 0.01 | 0.01 | 3e-6 | 0.01 | 3e-6 | 0.01 | 3e-6 |
| | BPIC20 _{int} | 0.15 | 0.05 | 0.01 | 2e-6 | 0.01 | 5e-6 | 0.01 | 2e-6 |
| | BPIC20 _{pre} | 0.09 | 0.03 | 0.01 | 5e-6 | 0.01 | 1e-7 | 0.01 | 1e-7 |
| | BPIC20 _{req} | 0.02 | 0.01 | 0.01 | 5e-6 | 0.01 | 5e-6 | 0.01 | 1e-7 |
| | BPIC20 _{tra} | 1.40 | 0.96 | 0.04 | 4e-6 | 0.30 | 3e-6 | 1.87 | 3e-6 |
| Sepsis | 0.19 | 0.65 | 0.13 | 1e-5 | 0.54 | 1e-5 | 2.61 | 4e-5 | |

cases. In this paper, we study the applicability of the proposals for scenarios where the expected number of cases to process simultaneously amounts to a few thousand. Accordingly, we present the runtime of *PrefAl* as the average of the first 1,000 processed cases. For the n -gram index proposal, we report separately the creation of the reachability graph and n -gram index (offline phase) and the average time required to process one ongoing case (online phase).

In the online phase, our proposal achieves a throughput of around 100 000 cases per second, while *PrefAl* ranges from 0.33 to 50 cases per second, with an average of 2 cases per second. Furthermore, in BPIC18 and BPIC19, we stopped the execution of *PrefAl* after 2 hours as it had processed less than 20 cases. Regarding the offline phase, the reachability graph is built in less than 1 second in most cases, and less than 5 minutes in the worst case. The n -gram indexes are generally computed in less than 15 seconds, with 1.5 hours in the worst case, in which the index for a lower n presented only 0.02 less accuracy, and took less than 4 minutes to build.

Threats to validity. The reported evaluation is potentially

affected by the following threats to validity. First, regarding *external validity*, the experiments rely only on six simulated and twelve real-life processes. The results could be different for other datasets. We have mitigated this threat by selecting datasets from processes across different domains. Second, regarding *construct validity*, in the real-life evaluation, we used a measure of goodness based on the enablement of the next recorded activity. The results could be different with other measures, e.g., considering the “*replayability*” of the remaining case rather than only the next activity.

VI. CONCLUSION AND FUTURE WORK

We presented a method to compute the state of an ongoing case w.r.t. a process model in constant time, based on the last n activities in the case’s trace prefix. Given a process model, the method generates a reachability graph and builds an n -gram index that associates each sequence of n (or fewer) consecutive activities generated by the model, with the state(s) in the reachability graph that this n -gram leads to. This n -gram index is computed offline and stored as a hash table. At

runtime, the state of an ongoing case, given its trace prefix, is computed in constant time by searching for the last n activities of the prefix, or the last $m < n$ activities, if this search fails.

The synthetic evaluation showed that our proposal is less affected by noise than the *PrefAl* baseline, as it only works with the last n executed activities. However, our proposal may fail to compute the correct state in complex processes. On the real-life logs, our method achieves a throughput of hundreds of thousands of cases per second, with an accuracy comparable to or above the baseline, w.r.t. its ability to correctly predict that the next activity is enabled in the returned state. These results hint that, in real-life processes, the next activities of an ongoing case depend more on the recently observed activities than on activities at the start of a case.

We also studied the problem of computing a reachability graph of a process model considering lazy vs. eager policies for gateway traversal. We proposed an algorithm to compute a reachability graph that allows for the replay of fitting traces in linear time, and evaluated this approach by replaying more than one million aligned cases of twelve real-life logs.

When the ending n -gram of a trace prefix cannot be found, we iteratively search for smaller m -grams ($m < n$). This is, in essence, an approach to finding a partial n -gram match. In future work, we plan to experiment with partial n -gram matching techniques to retrieve the closest matching n -gram(s). A partial matching approach could also help us to reduce the number of n -grams we need to index. Searching in the index with small variations of this n -gram may lead to a better result when the n -gram does not have a match itself, or reduce the number of states when the n -gram itself returns a big number of them. We also plan to study the possibility of storing the reachability graph in a graph database, and query directly for the markings that are at the end of an arc sequence with the n -gram as labels. This would sacrifice runtime, but avoid the need to compute and store the n -gram index.

Reproducibility The method's implementation and scripts to reproduce the experiments are available at: <https://github.com/AutomatedProcessImprovement/process-running-state/tree/IEEEETSC>. The datasets and evaluation results are available at: <https://zenodo.org/doi/10.5281/zenodo.11409896>.

ACKNOWLEDGEMENTS

This research is funded by the Estonian Research Council (PRG1226).

REFERENCES

- [1] W. M. P. van der Aalst, *Process Mining - Data Science in Action, Second Edition*. Springer, 2016.
- [2] M. de Leoni, S. Suriadi, A. H. M. ter Hofstede, and W. M. P. van der Aalst, "Turning event logs into process movies: animating what has really happened," *Softw. Syst. Model.*, vol. 15, no. 3, pp. 707–732, 2016.
- [3] M. T. Wynn, M. Dumas, C. J. Fidge, A. H. M. ter Hofstede, and W. M. P. van der Aalst, "Business process simulation for operational decision support," in *BPM 2007 Workshops*, ser. LNCS, vol. 4928. Springer, 2007, pp. 66–77.
- [4] H. A. Reijers and W. M. P. van der Aalst, "Short-term simulation: bridging the gap between operational control and strategic decision making," in *Proceedings of the 10th IASTED International Conference on Modelling and Simulation (MS)*. IASTED/Acta Press, 1999, pp. 417–421.
- [5] A. Rozinat, M. T. Wynn, W. M. P. van der Aalst, A. H. M. ter Hofstede, and C. J. Fidge, "Workflow simulation for operational decision support," *Data Knowl. Eng.*, vol. 68, no. 9, pp. 834–850, 2009.
- [6] A. Adriansyah, B. F. van Dongen, and W. M. P. van der Aalst, "Conformance checking using cost-based fitness analysis," in *Proceedings of the 15th IEEE International Enterprise Distributed Object Computing Conference (EDOC)*. IEEE Computer Society, 2011, pp. 55–64.
- [7] A. Berti and W. M. P. van der Aalst, "A novel token-based replay technique to speed up conformance checking and process enhancement," *Trans. Petri Nets Other Model. Concurr.*, vol. 15, pp. 1–26, 2021.
- [8] D. Schuster and S. J. van Zelst, "Online process monitoring using incremental state-space expansion: An exact algorithm," in *Proceedings of the 18th International Conference on Business Process Management (BPM)*, ser. LNCS, vol. 12168. Springer, 2020, pp. 147–164.
- [9] W. M. P. van der Aalst, "Workflow verification: Finding control-flow errors using petri-net-based techniques," in *Business Process Management, Models, Techniques, and Empirical Studies*, ser. LNCS, vol. 1806. Springer, 2000, pp. 161–183.
- [10] C. Favre, D. Fahland, and H. Völzer, "The relationship between workflow graphs and free-choice workflow nets," *Inf. Syst.*, vol. 47, pp. 197–219, 2015.
- [11] S. J. van Zelst, A. Bolt, M. Hassani, B. F. van Dongen, and W. M. P. van der Aalst, "Online conformance checking: relating event streams to process models using prefix-alignments," *Int. J. Data Sci. Anal.*, vol. 8, no. 3, pp. 269–284, 2019.
- [12] K. Raun, M. Nielsen, A. Burattin, and A. Awad, "C-3PA: streaming conformance, confidence and completeness in prefix-alignments," in *Proceedings of the 35th International Conference on Advanced Information Systems Engineering (CAISE)*, ser. LNCS, vol. 13901. Springer, 2023, pp. 437–453.
- [13] J. Carmona, B. F. van Dongen, A. Solti, and M. Weidlich, *Conformance Checking - Relating Processes and Models*. Springer, 2018.
- [14] W. Song, X. Xia, H. Jacobsen, P. Zhang, and H. Hu, "Efficient alignment between event logs and process models," *IEEE Trans. Serv. Comput.*, vol. 10, no. 1, pp. 136–149, 2017.
- [15] B. F. van Dongen, J. Carmona, T. Chatain, and F. Taymouri, "Aligning modeled and observed behavior: A compromise between computation complexity and quality," in *Proceedings of the 29th International Conference on Advanced Information Systems Engineering (CAISE)*, ser. LNCS, vol. 10253. Springer, 2017, pp. 94–109.
- [16] A. Syamsiyah and B. F. van Dongen, "Improving alignment computation using model-based preprocessing," in *Proceedings of the 1st International Conference on Process Mining (ICPM)*. IEEE, 2019, pp. 73–80.
- [17] A. Burattin, S. J. van Zelst, A. Armas-Cervantes, B. F. van Dongen, and J. Carmona, "Online conformance checking using behavioural patterns," in *Proceedings of the 16th International Conference on Business Process Management (BPM)*, ser. LNCS, vol. 11080. Springer, 2018, pp. 250–267.
- [18] W. L. J. Lee, A. Burattin, J. Munoz-Gama, and M. Sepúlveda, "Orientation and conformance: A hmm-based approach to online conformance checking," *Inf. Syst.*, vol. 102, p. 101674, 2021.
- [19] H. Völzer, "A new semantics for the inclusive converging gateway in safe processes," in *Proceedings of the 8th International Conference on Business Process Management (BPM)*, ser. LNCS, vol. 6336. Springer, 2010, pp. 294–309.
- [20] A. Berti, S. J. van Zelst, and D. Schuster, "Pm4py: A process mining library for python," *Softw. Impacts*, vol. 17, p. 100556, 2023.
- [21] S. J. J. Leemans, D. Fahland, and W. M. P. van der Aalst, "Discovering block-structured process models from event logs containing infrequent behaviour," in *BPM 2013 Workshops*, ser. LNBIP, vol. 171. Springer, 2013, pp. 66–78.